Nonlocal Interface Dynamics and Pattern Formation in Gravity-Driven Unsaturated Flow through Porous Media

Luis Cueto-Felgueroso and Ruben Juanes*

Massachusetts Institute of Technology, 77 Massachusetts Ave, Building 48–319, Cambridge Massachusetts 02139, USA

(Received 31 July 2008; published 12 December 2008)

Existing continuum models of multiphase flow in porous media are unable to explain why preferential flow (fingering) occurs during infiltration into homogeneous, dry soil. Following a phase-field methodology, we propose a continuum model that accounts for an apparent surface tension at the wetting front and does not introduce new independent parameters. The model reproduces the observed features of fingered flows, in particular, the higher saturation of water at the tip of the fingers, which is believed to be essential for the formation of fingers. From a linear stability analysis, we predict that finger velocity and finger width both increase with infiltration rate, and the predictions are in quantitative agreement with experiments.

DOI: 10.1103/PhysRevLett.101.244504 PACS numbers: 47.56.+r, 47.20.−k, 47.54.−r, 47.55.nb

The unstable displacement of a fluid by another fluid in a porous medium is a fascinating example of pattern formation in nonlinear dissipative systems [1–3]. The rich variety of macroscopic invasion patterns stems from a delicate interaction between capillary, viscous and gravitational forces at the pore scale. In gravity-driven infiltration into initially dry, homogeneous soil, the resulting pattern often takes the form of preferential flow paths (fingers), which have been consistently observed in laboratory and field experiments for nearly half a century [4,5]. Fingering leads to smaller residence times of contaminants in soil, may play an important role in soil weathering at the time scale of millennia [6], and it may be crucial to the impact of water dropout on the operational efficiency of polymer electrolyte fuel cells [7].

Despite the frequent occurrence of gravity fingers in unsaturated media, the explanation, modeling and prediction of fingered flows with continuum (macroscopic) mathematical models has remained elusive. Many authors have approached the wetting front instability by drawing an analogy with the two-fluid system in a Hele-Shaw cell [8], and their analyses have led to kinematic models that reproduce trends observed in the experiments, such as relations between finger width and finger tip velocity with the flow rate through the finger [5,9–12]. Simulation of unstable gravity flows has also been performed with modified invasion-percolation models at the pore scale [13,14].

By contrast, conservation laws that model the evolution of water saturation S (that is, the locally averaged fraction of pore space occupied by water) have been, so far, unable to model gravity fingering successfully. The traditional model of unsaturated flow, known as Richards equation [15], is a mass balance equation in which the water flux is modeled by a straightforward extension of Darcy's law to unsaturated media. It accounts for gravity, capillarity, and the fact that the permeability to water is reduced because the porous medium is only partially saturated with water. It is well known that Richards equation leads to monotonic saturation profiles and cannot predict or simulate fingering under any conditions [16].

To remedy this behavior, several extensions to Richards equation have been proposed. These include a formulation with dynamic capillary pressure [16,17], designed to account for additional terms that arise from averaging of the microscopic multiphase flow equations. A related model [18] contains a hypodiffusive term, introduced to mimic the observed hold-back–pile-up effect, which gives rise to a saturation overshoot at the wetting front—a distinctive feature of fingered flows. Higher-order terms are required, however, to regularize the mathematical problem [19]. Here, we propose a physical mechanism and a subsequent continuum mathematical model that explain why gravity fingers occur during infiltration, and predict when and how they will grow.

Consider constant-flux infiltration into a porous medium (Fig. 1). It is assumed that the initial water saturation S_0 is uniform, and that the infiltration rate R_F is uniformly distributed and constant in time. The z-spatial coordinate points downwards, in the direction of gravity (acceleration g). The water density and dynamic viscosity are ρ and μ. The relevant (macroscopic) parameters concerning the porous medium are its intrinsic permeability k, and its porosity ϕ. The permeability of the medium is often expressed as a saturated hydraulic conductivity, $K_s = k\rho g/\mu$, which equals the gravity-driven flux under full saturation. Hence, the infiltration rate R_F may be expressed as a flux ratio, $R_s = R_F/K_s$, with $R_s \in [0, 1]$. When this idealized flow scenario is simulated experimentally, the stability of the wetting front seems to be controlled by the flux ratio, initial saturation and material nonlinearity [18]. A saturation overshoot is observed at the tip of the fingers, which grow as traveling waves, advancing with constant velocity [20]. The formation of fingers appears as a winner-takes-all process, by which the fastest growing fingers in the initial unstable front channelize most of the infiltrating fluid and inhibit the growth of other incipient

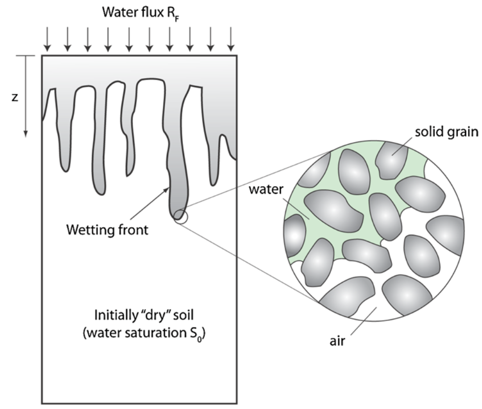

FIG. 1 (color online). Schematic of vertical infiltration of water into a porous medium. Initially, the soil is almost dry (water saturation S_0). A constant and uniformly distributed flux of water R_F (LT^{-1}) infiltrates into the soil. The flux of water is less than the hydraulic conductivity of the soil, K_s, so that the flux ratio $R_s = R_F/K_s < 1$. Macroscopically, a diffuse interface (the wetting front) moves downwards. This interface is often unstable and takes the form of long and narrow fingers that travel faster than the base of the wetting front (see, e.g., Fig. 2 in [5]). Microscopically, a sharp interface between water and air exists (see inset), which is locally governed by capillary effects.

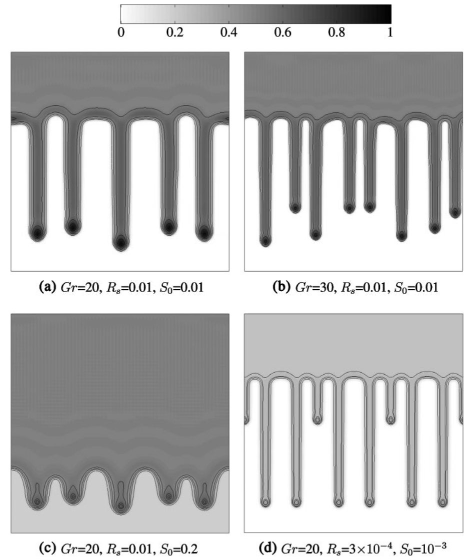

FIG. 2. Saturation maps from the numerical simulations of Eq. (2), for different values of the gravity number Gr, flux ratio R_s, and initial saturation S_0. The computational domain is the square $[-1, 1] \times [-1, 1]$. Increasing the gravity number [(a) and (b)] changes the scale of the problem but not the nonlinear dynamics of the wetting front. Large initial saturations (c) lead to a compact invasion, and small flux ratios (d) produce thinner, slower fingers in sufficiently dry media. The flow dynamics and the distinctive saturation overshoot at the tip of the fingers, which behave as traveling waves, agree with experimental observations.

fingers [5,20]. The initial moisture content plays a critical role in the fingering instability: even relatively low saturations lead to a compact, downward-moving wetting front [21]. Stable fronts are also observed in dry media when the infiltration rate is either very small or approaches the saturated conductivity. In general, larger infiltration rates produce faster, thicker fingers [5].

The free energy of the system, which is assumed to be incompressible, is characterized in dimensionless quantities by the functional

$$\mathcal{E} = \int \Big(\underbrace{-Sz + \mathrm{Gr}^{-1}\psi(S)}_{\text{local}} + \underbrace{\frac{1}{2} N\ell |\nabla S|^2}_{\text{nonlocal}} \Big) d\mathbf{x}, \qquad (1)$$

where Gr and $N\ell$ are two dimensionless groups. The above functional comprises the gravitational and capillary pressure potentials, as well as a nonlocal energy potential, which models the extra energetic cost associated with the displacement of water-air interfaces in areas of large saturation gradients. This last term is formally equivalent to an apparent surface tension associated to the wetting front. Mass conservation and gradient flow based on the energy functional in Eq. (1) lead to the evolution equation for the water saturation S,

$$\frac{\partial S}{\partial t} + \nabla \cdot \{k_r(S)[\nabla z + \mathrm{Gr}^{-1}\nabla J(S) + N\ell \nabla(\Delta S)]\} = 0. \qquad (2)$$

Our model is similar to that describing the flow of thin films [22,23], and to phase-field models of epitaxial growth of surfaces and binary transitions [24,25]. The traditional Richards equation can be recovered by neglecting the nonlocal energy term in Eq. (2). We define the saturation-dependent relative permeability $k_r(S)$ and the dimensionless capillary pressure $J(S) = -\psi'(S)$. The functional forms of these constitutive relations are chosen to fit experimental data from quasistatic experiments. In the following, we adopt the van Genuchten–Mualem model [26],

$$k_r(S) = \sqrt{S}[1 - (1 - S^{1/m})^m]^2, \qquad J(S) = (S^{-1/m} - 1)^{1/n}, \qquad (3)$$

where $m = 1 - 1/n$. This model introduces two intrinsic material parameters: α and n. The dimension of α is L^{-1}, and α^{-1} is approximately the capillary rise. The nonlinearity of the material is determined by n, which depends on how well-sorted the porous medium is. The gravity number Gr is defined as $\mathrm{Gr} = \alpha L$, where L is an *arbitrary* length scale used to nondimensionalize the equations. The dependence of the capillary rise on the system parameters is given by the Leverett scaling $h_{\mathrm{cap}} \sim \alpha^{-1} \sim \gamma \cos\theta / (\rho g \sqrt{k/\phi})$, where γ is the surface tension between the fluids, and θ is the contact angle between the air-water interface and the solid surface [27].

Dimensional analysis leads to the scalings $\mathrm{Gr} \sim L$ and $N\ell \sim L^{-3}$, which simply reflect that the solution should be independent of the choice of the reference length scale L. In principle, one might postulate the dependence of $N\ell$ on an additional intrinsic property of the system. Since the idea of a nonlocal interface is fundamentally a macroscopic construct, it is more rigorous to express $N\ell$ in terms of the already considered basic parameters, and thus arrive at the scaling $N\ell \sim \mathrm{Gr}^{-3}$. The coefficient linking $N\ell$ and Gr^{-3} must be a constant, and simple analysis suggests that its magnitude is of the order of 1. Therefore, we propose the relation

$$N\ell = \mathrm{Gr}^{-3}. \tag{4}$$

As a consequence of Eq. (4), the gravity number Gr sets the intrinsic scale of the problem, and the proposed model contains a new term, but not a new independent parameter.

The numerical solutions to Eq. (2) capture the experimentally observed features of preferential flow and wetting front instability (Fig. 2). The most salient qualitative discrepancy between the numerical simulations and the experimental visualizations is the absence of meandering of the fingers, which is due to small heterogeneities and packing irregularities that always exist in the experiments and are not considered in the simulations. Our model permits investigation of the dependence of the flow characteristics with the various system parameters, and predicts the existence of a saturation ridge along the finger root front, which should be analyzed in future experiments.

The linear stability analysis of Eq. (2) provides further insight into the role of the system parameters on the dynamics of the flow. Stability refers here to the growth or decay of planar infinitesimal perturbations to the traveling wave solutions to Eq. (2). We distinguish between asymptotic (modal) and transient (nonmodal) growth behavior, the latter arising from the non-normality of the linearized flow operator [23,28]. For each set of parameters, we determine the frequency $\omega_{\max}$ of the most unstable mode, as well as its associated asymptotic growth factor $\beta_{\max}$ and the transient growth behavior. Positive values of $\beta_{\max}$ or intense transient growth are indicative of an unstable wetting front, and their magnitudes correlate with the severity of fingering.

When the dimensionless groups Gr and $N\ell$ are considered independent, there is a narrow region in the parameter space Gr–$N\ell$ where $\omega_{\max}$ [Fig. 3(a)] and $\beta_{\max}$ [Fig. 3(b)] decay exponentially. This region of abrupt decay marks the effective transition from a compact infiltration front to fingering instability, and follows a straight line (in logarithmic scale) of slope -3. The specific location of the transition (not its slope) is determined by the system parameters R_s, S_0 and n. This critical region cannot be crossed when Gr moves along $N\ell = \mathrm{Gr}^{-3}$, and therefore changes in the gravity number do not induce regime transition.

The stability analysis also reveals that, under the scaling $N\ell = \mathrm{Gr}^{-3}$, $\omega_{\max}$ and $\beta_{\max}$ are linear functions of Gr. The scale-invariant frequencies and growth factors, $\omega_{\max}/\mathrm{Gr}$ [Fig. 3(c)] and $\beta_{\max}/\mathrm{Gr}$ [Fig. 3(d)], are indicative of the early dynamics of the perturbed flow and the properties of the emerging fingers. The onset of preferential flow paths in the unstable wetting front is more intense for larger flux ratios and smaller initial saturations. For very dry media the size of the incipient fingers decreases with the flux ratio. In general, however, for each value of the initial saturation there is a critical flux ratio beyond which smaller fluxes lead to larger finger sizes [Fig. 3(c)]. This nontrivial result shows that it is possible to observe both decrease and increase in finger size with decreasing R_s, depending on the particular values of R_s and S_0. The growth factor and frequency of the most unstable mode decay exponentially as the initial saturation is increased. This abrupt decay agrees with experimental observations, which have suggested the existence of critical values of S_0 for the suppression of the instability [21].

A linear stability analysis has applicability, strictly speaking, to incipient perturbation growth. The dominant role of the fastest growing fingers suggests, however, that the results of a modal analysis may correlate with the

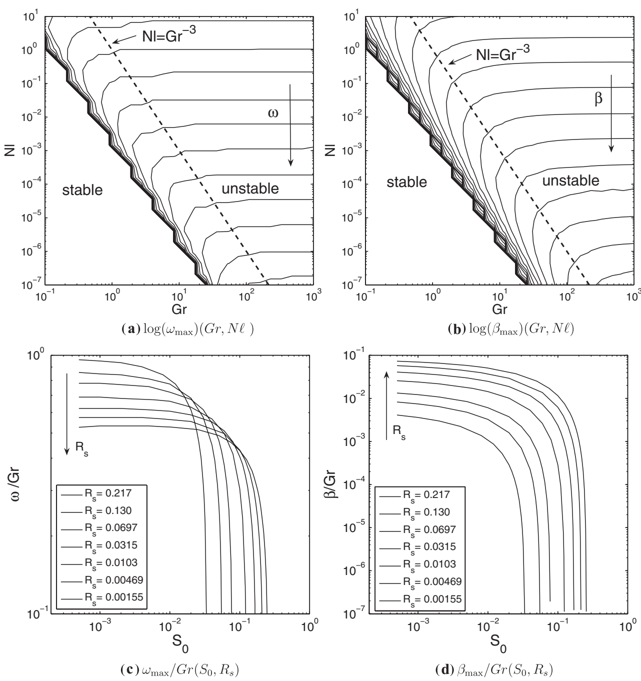

FIG. 3. Results of the linear stability analysis of Eq. (2). (a)–(b) Contours of the logarithm of the frequency $\omega_{\max}$ of the most unstable mode and its associated growth factor $\beta_{\max}$, as functions of the dimensionless groups Gr and $N\ell$. We set $R_s = 0.217$, $S_0 = 0.01$ and $n = 10$. A narrow region of exponential decay, along a straight line of slope -3, marks the effective transition from stable to unstable flow. The position of this transition region, not its slope, is determined by R_s, S_0 and n. Under the proposed scaling $N\ell = \mathrm{Gr}^{-3}$, the transition region cannot be crossed by modifying Gr alone. (c) Exponential decay of the scale-invariant frequencies $\omega_{\max}/\mathrm{Gr}$ with the initial saturation S_0. For a given S_0, the frequencies increase with decreasing R_s, up to a critical flux beyond which $\omega_{\max}/\mathrm{Gr}$ decreases again. (d) Exponential decay of the scale-invariant growth factor $\beta_{\max}/\mathrm{Gr}$ with the initial saturation S_0. Within the unsaturated regime, the growth factors increase monotonically with R_s.

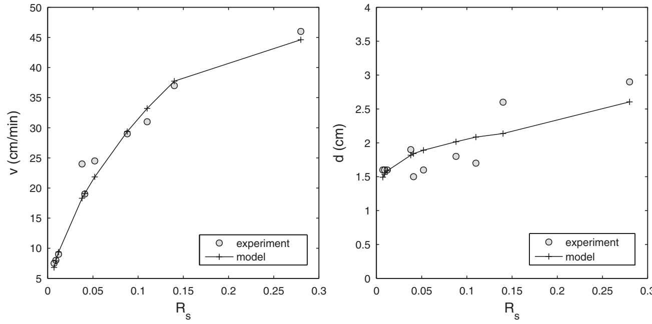

(a) Finger velocity **(b)** Finger width

FIG. 4. Average finger tip velocity (a) and finger width (b) versus flux ratio R_s. The circles are the experimental measurements of Glass *et al.* [5]. The crosses (joined by straight solid lines) are the values predicted by the linear stability analysis, together with Eq. (5). We set $S_0 = 0.0003$, $n = 10$, and a gravity number $\mathrm{Gr} = 50$ based on the height of the experimental chamber. The constants in Eq. (5) are estimated as $\mathcal{C}_v = 6.8$ and $\mathcal{C}_d = 0.9$. The predictions based on the linear stability analysis reproduce the observed increase of finger velocity and finger size with the flux ratio.

characteristics of the fully developed fingers. Using dimensional analysis, and assuming that the finger properties can be determined from the basic system parameters and the dimensionless groups $\beta_{\max}$, $\omega_{\max}$ and Gr, we arrive at the following expressions for finger tip velocity v and finger width d:

$$v = \mathcal{C}_v \frac{K_s}{\phi} \frac{\beta_{\max}}{\mathrm{Gr}}, \qquad d = \mathcal{C}_d \alpha^{-1} \left(\frac{\omega_{\max}}{Gr} \right)^{-1}, \qquad (5)$$

where $\mathcal{C}_v$ and $\mathcal{C}_d$ are experimental constants. For initially dry media, the flux ratio has a relatively modest influence on $\omega_{\max}$ [Fig. 3(c)], and therefore Eq. (5) predicts that the finger width roughly scales like $d \sim h_{\mathrm{cap}}$, which is consistent with experimental observations and scaling theories in porous media [29].

To test these predictions, we compare the finger properties given by Eq. (5) with measurements from the experiments by Glass *et al.* [5]. They report experiments of infiltration into homogeneous, initially dry, coarse sands, for different flux ratios. Constant infiltration rates are achieved through the use of a two-layer configuration, with a tall, coarse-sand layer at the bottom of the chamber, and a thinner, less conductive, fine-sand layer on top. Comparison of the experimental and predicted finger characteristics (Fig. 4) suggests the choices $\mathcal{C}_v = 6.8$ and $\mathcal{C}_d = 0.9$. The results from the linear stability analysis, together with Eq. (5), not only reproduce the observed trends in finger velocity [Fig. 4(a)] and finger width [Fig. 4(b)], but also show good quantitative agreement with the experimental measurements.

The present study shows that gravity fingering in unsaturated flow can be explained, described and modeled by means of continuum balance laws. The success of this simple model to explain infiltration fingers suggests that similar continuum models, derived using the framework of phase-field modeling, may improve our ability to predict unstable multiphase flow in porous media.

We gratefully acknowledge funding for this research, provided by Eni under the Multiscale Reservoir Science project, and by the Winslow Career Development Chair.

*juanes@mit.edu

[1] J. P. Gollub and J. S. Langer, Rev. Mod. Phys. **71**, S396 (1999).
[2] R. Lenormand, Physica (Amsterdam) **140A**, 114 (1986).
[3] M. Sahimi, Rev. Mod. Phys. **65**, 1393 (1993).
[4] D. E. Hill and J.-Y. Parlange, Soil Sci. Soc. Am. J. **36**, 397 (1972).
[5] R. J. Glass, J.-Y. Parlange, and T. S. Steenhuis, Water Resour. Res. **25**, 1195 (1989).
[6] D. Markewitz, E. A. Davidson, R. Figueiredo, R. L. Victoria, and A. V. Krusche, Nature (London) **410**, 802 (2001).
[7] C. Y. Wang, Chem. Rev. **104**, 4727 (2004).
[8] P. G. Saffman and G. I. Taylor, Proc. R. Soc. A **245**, 312 (1958).
[9] R. L. Chuoke, P. van Meurs, and C. van der Poel, Petrol. Trans. Am. Inst. Min. Eng. **216**, 188 (1959).
[10] J.-Y. Parlange and D. E. Hill, Soil Science **122**, 236 (1976).
[11] D. A. Weitz, J. P. Stokes, R. C. Ball, and A. P. Kushnick, Phys. Rev. Lett. **59**, 2967 (1987).
[12] D. A. DiCarlo and M. J. Blunt, Water Resour. Res. **36**, 2781 (2000).
[13] B. Xu, Y. C. Yortsos, and D. Salin, Phys. Rev. E **57**, 739 (1998).
[14] B. Berkowitz and R. P. Ewing, Rev. Geophys. **19**, 23 (1998).
[15] L. A. Richards, Physics (N.Y.) **1**, 318 (1931).
[16] J. L. Nieber, R. Z. Dautov, A. G. Egorov, and A. Y. Sheshukov, Transp. Porous Media **58**, 147 (2005).
[17] S. M. Hassanizadeh and W. G. Gray, Water Resour. Res. **29**, 3389 (1993).
[18] M. Eliassi and R. J. Glass, Water Resour. Res. **38**, 1234 (2002).
[19] D. A. DiCarlo, R. Juanes, T. LaForce, and T. P. Witelski, Water Resour. Res. **44**, W02406 (2008).
[20] J. S. Selker, J.-Y. Parlange, and T. Steenhuis, Water Resour. Res. **28**, 2523 (1992).
[21] T. X. Lu, J. W. Biggar, and D. R. Nielsen, Water Resour. Res. **30**, 3283 (1994).
[22] H. E. Huppert, Nature (London) **300**, 427 (1982).
[23] A. L. Bertozzi and M. P. Brenner, Phys. Fluids **9**, 530 (1997).
[24] M. Dubé, M. Rost, K. R. Elder, M. Alava, S. Majaniemi, and T. Ala-Nissila, Phys. Rev. Lett. **83**, 1628 (1999).
[25] H. Emmerich, Adv. Phys. **57**, 1 (2008).
[26] M. T. van Genuchten, Soil Sci. Soc. Am. J. **44**, 892 (1980).
[27] P. G. de Gennes, Rev. Mod. Phys. **57**, 827 (1985).
[28] L. N. Trefethen, A. E. Trefethen, S. C. Reddy, and T. A. Driscoll, Science **261**, 578 (1993).
[29] J. S. Selker and M. H. Schroth, Water Resour. Res. **34**, 1935 (1998).